

AperTO - Archivio Istituzionale Open Access dell'Università di Torino

**Photochemical transformation of benzotriazole, relevant to sunlit surface waters: Assessing the possible role of triplet-sensitised processes**

**This is the author's manuscript**

*Original Citation:*

*Availability:*

This version is available <http://hdl.handle.net/2318/1615931> since 2017-01-17T16:48:56Z

*Published version:*

DOI:10.1016/j.scitotenv.2016.05.119

*Terms of use:*

Open Access

Anyone can freely access the full text of works made available as "Open Access". Works made available under a Creative Commons license can be used according to the terms and conditions of said license. Use of all other works requires consent of the right holder (author or publisher) if not exempted from copyright protection by the applicable law.

(Article begins on next page)

This Accepted Author Manuscript (AAM) is copyrighted and published by Elsevier. It is posted here by agreement between Elsevier and the University of Turin. Changes resulting from the publishing process - such as editing, corrections, structural formatting, and other quality control mechanisms - may not be reflected in this version of the text. The definitive version of the text was subsequently published in SCIENCE OF THE TOTAL ENVIRONMENT, 566-567, 2016, 10.1016/j.scitotenv.2016.05.119.

You may download, copy and otherwise use the AAM for non-commercial purposes provided that your license is limited by the following restrictions:

- (1) You may use this AAM for non-commercial purposes only under the terms of the CC-BY-NC-ND license.
- (2) The integrity of the work and identification of the author, copyright owner, and publisher must be preserved in any copy.
- (3) You must attribute this AAM in the following format: Creative Commons BY-NC-ND license (<http://creativecommons.org/licenses/by-nc-nd/4.0/deed.en>), 10.1016/j.scitotenv.2016.05.119

The publisher's version is available at:

<http://linkinghub.elsevier.com/retrieve/pii/S004896971631049X>

When citing, please refer to the published version.

Link to this full text:

<http://hdl.handle.net/2318/1615931>

# Photochemical transformation of benzotriazole, relevant to sunlit surface waters: Assessing the possible role of triplet-sensitised processes

Angelica Bianco,<sup>a</sup> Debora Fabbri,<sup>b</sup> Marco Minella,<sup>b</sup> Marcello Brigante,<sup>a,c,\*</sup> Gilles Mailhot,<sup>a,c</sup> Valter Maurino,<sup>b</sup> Claudio Minero,<sup>b</sup> Davide Vione<sup>b,d,\*</sup>

<sup>a</sup> Clermont Université, Université Blaise Pascal, Institut de Chimie de Clermont-Ferrand, BP 10448, F-63000 Clermont-Ferrand, France.

<sup>b</sup> Università degli Studi di Torino, Dipartimento di Chimica, Via P. Giuria 5, 10125 Torino, Italy. <http://www.chimicadellambiente.unito.it>

<sup>c</sup> CNRS, UMR 6296, ICCF, BP 80026, F-63177 Aubière, France.

<sup>d</sup> Università degli Studi di Torino, Centro Interdipartimentale NatRisk, Via L. Da Vinci 44, 10095 Grugliasco (TO), Italy. <http://www.natrisk.org>

\* Address correspondence to either author: [marcello.brigante@univ-bpclermont.fr](mailto:marcello.brigante@univ-bpclermont.fr); [davide.vione@unito.it](mailto:davide.vione@unito.it)

## Abstract

The corrosion inhibitor 1H-Benzotriazole ( $pK_a = 8.4$ ) can exist in two different forms in natural waters, and photochemical transformation is a potentially significant attenuation pathway for both of them. Depending on conditions, the modelled half-life times range from some days/weeks to several months. In sunlit water bodies, the acidic (neutral) form would undergo direct photolysis (accounting for up to 7% of total phototransformation) and, most notably, reaction with the hydroxyl radicals ( $\bullet\text{OH}$ ) and the triplet states of chromophoric dissolved organic matter ( ${}^3\text{CDOM}^*$ ). The basic (anionic) form would undergo significant transformation with  $\bullet\text{OH}$  and  ${}^3\text{CDOM}^*$ . The  $\bullet\text{OH}$  reactions would be more important at low dissolved organic carbon (DOC) and the  ${}^3\text{CDOM}^*$  processes at high DOC. In the presence of reactive triplet-state model compounds, the two benzotriazole forms react with similar rate constants. In this case, they would show comparable half-life times in surface-water environments. With less reactive triplet states, the rate constant of the anionic form can be a couple of orders of magnitude higher than that of the neutral one. Under these circumstances, the neutral form could be considerably more photostable than the anionic one at high DOC. Therefore, depending on  ${}^3\text{CDOM}^*$  reactivity, the solution pH may or may not play an important role in the photoattenuation kinetics of 1H-benzotriazole in sunlit natural waters, especially at high DOC. Both forms of benzotriazole yield hydroxyderivatives as their main transformation intermediates under all the relevant photochemical reaction pathways. These intermediates could be formed via  $\bullet\text{OH}$ -induced hydroxylation, or upon electron abstraction followed by reaction with water. Differently from UVC irradiation data reported in previous studies, the concentration of aniline upon excitation of 1H-benzotriazole under environmentally

significant UV wavelengths was always below the detection limit of the analytical method used in this work ( $5 \mu\text{mol L}^{-1}$ ).

**Keywords:** Environmental fate; Organic pollutants; Transformation intermediates; Triplet states; 1H-Benzotriazole; Photochemical attenuation.

## Introduction

Benzotriazole (1H-Benzotriazole or 1,2,3-Benzotriazole, hereafter BZT) is a heterocyclic compound acting as an effective corrosion inhibitor, particularly for copper and its alloys. This property accounts for the widespread BZT use, not only in the direct protection of metal surfaces but also as an additive for several substances and materials that could come in contact with metals during use. A partial list of products that can contain BZT includes lacquer and varnishes, waxes and polish, packing papers, lubricants, brake fluids, sealants, detergents for metals, as well as aircraft de-icing fluids. BZT is also used as an additive in recirculating water for engine cooling, air conditioning, heating systems, and industrial equipment (Allam et al., 2009; Finsgar and Milosev, 2010; Copper Development Association, 2016). Moreover, the biological activity of BZT and its derivatives makes them a useful library of potential drug precursors (Briguglio et al., 2015).

Unfortunately, BZT is quite persistent in the environment which, combined with its widespread use, has resulted in the non-surprising detection of this compound in a variety of environmental matrices including soil, sediment, surface and ground water, and snow (Giger et al., 2006; Alotaibi et al., 2015; Careghini et al., 2015). In particular, the occurrence of BZT in wastewater is mainly due to its inclusion in household detergent formulations, and dishwashers effluents account for the majority of BZT emissions to wastewater (Vetter and Lorenz, 2013). The biorefractory nature of BZT and related compounds accounts for their incomplete removal by wastewater treatment plants (Morasch et al., 2010; Reemtsma et al., 2010; Herzog et al., 2014; Acero et al., 2015; Molins-Delgado et al., 2015), with consequent release to the receiving water bodies. An additional source is caused by the use of BZT in aircraft de-icing formulations, with possible contamination of soil and groundwater near airports (McNeill and Cancilla, 2009; Sulej et al., 2013).

Biodegradation of BZT is possible but it is rather slow, with reported half-life times ranging from one month to almost one year and, sometimes, no degradation at all (Liu et al., 2011; Liu et al., 2013; Alotaibi et al., 2015). Photodegradation is a potentially competitive transformation pathway for BZT in surface waters (Matamoros et al., 2010; Janssen et al., 2015). Photoinduced transformation is usually divided into direct photolysis, where a contaminant absorbs sunlight and undergoes transformation as a consequence (Aguera et al., 2012), and indirect photochemistry. In the latter, sunlight is absorbed by photoactive molecules called photosensitisers, which in surface waters include chromophoric dissolved organic matter (CDOM), nitrate and nitrite. Irradiated photosensitisers produce reactive transients species such as hydroxyl radicals ( $\bullet\text{OH}$ ), singlet oxygen

( $^1\text{O}_2$ ) and CDOM triplet states ( $^3\text{CDOM}^*$ ), which are involved in pollutant transformation (Takeda et al., 2004; Nakatani et al., 2007; Lee et al., 2013; Vione et al., 2014; Chiwa et al., 2015). The combination of direct and indirect photochemistry can induce effective pollutant degradation in a variety of environmental conditions, but it can also generate harmful transformation intermediates (DellaGreca et al., 2004; Carlos et al., 2012; Wang and Lin, 2012; Anger et al., 2013).

In the case of BZT phototransformation, an issue of considerable concern is the detection of aniline upon BZT direct photolysis (Hem et al., 2003; Benitez et al., 2013). Aniline has been detected upon UVC irradiation, and it is thus very important to check whether its formation from BZT is also possible under conditions that are representative of sunlit surface waters. The concern related to the possible formation of aniline is due to its being classified as a probable carcinogen for humans, based on its ability to induce spleen cancer in rats (EPA, 2000). The carcinogenicity of this compound has been the object of debate, and the link between aniline exposure and cancer development is probably not accounted for by primary genotoxicity, but rather by hematotoxicity and cell damage/proliferation effects (Bomhard and Herbold, 2005; Wang et al., 2015).

Another key issue connected with BZT phototransformation is that, while its direct photolysis quantum yields and reaction rate constants with  $\bullet\text{OH}$  and  $^1\text{O}_2$  are reported in the literature (Naik and Moorthy, 1995; Benitez et al., 2013; Janssen et al., 2015), no data are available concerning the BZT reactivity with  $^3\text{CDOM}^*$ . Unfortunately, natural CDOM is a very complex mixture of compounds and the experimental measurement of substrate reactivity with  $^3\text{CDOM}^*$  is very challenging. To simplify the experimental system, in this work we have used two CDOM proxies that behave as triplet sensitizers under irradiation. The chosen proxies are anthraquinone-2-sulphonate (AQ2S) and 1-nitronaphthalene (1NN). The main reasons for choosing AQ2S are the following: (i) quinones are photoactive CDOM components (Cory and McKnight, 2005; Fimmen et al., 2007; Clark et al., 2014) and (ii) AQ2S photochemistry is well known and it does not involve additional transient species such as  $\bullet\text{OH}$  or  $^1\text{O}_2$  (Bedini et al., 2012). Unfortunately, the AQ2S triplet state ( $^3\text{AQ2S}^*$ ) is often more reactive than average  $^3\text{CDOM}^*$  and it may represent an upper limit of triplet-sensitized photoreactivity induced by CDOM (De Laurentiis et al., 2014). Although 1NN bears little resemblance with CDOM functional groups, its triplet state ( $^3\text{1NN}^*$ ) is less reactive than  $^3\text{AQ2S}^*$ ; the standard reduction potentials of these triplet states are in fact 2 and 2.6 V, respectively (Loeff et al., 1993; Brigante et al., 2010; Sur et al., 2011; De Laurentiis et al., 2012). Therefore, results obtained with 1NN can be used to check for the AQ2S ones and provide a control for the rate constants of triplet sensitization. Moreover, 1NN is easy and convenient to use in laser flash photolysis experiments because its triplet state, absorbing radiation at both 380 and 620 nm, can be monitored in different wavelength intervals to overcome possible problems of spectral interferences (Brigante et al., 2010).

Based on previous considerations, the present work has the following goals: (i) predicting the kinetics of BZT photochemical transformation in surface-water bodies, as a function of the environmental variables, and (ii) assessing the possible formation of aniline upon BZT

phototransformation. To reach these goals, it was essential to get insight into the triplet-sensitised reactivity of BZT.

## Experimental

**Reagents and materials.** The chemicals used in this study were of at least analytical grade and used as received, without further purification. Organic solvents were of HPLC grade (Aldrich). Water used was of Milli-Q quality (resistivity >18.2 MΩ cm, total organic carbon < 2 ppb).

The benzotriazole molecule is a weak acid with pKa = 8.4 (Hansen et al., 1968). The neutral form (hereafter, HBZT) is expected to prevail in ~neutral pH conditions that are common in surface waters, but the anionic form (hereafter, BZT<sup>-</sup>) can play a significant or even predominant role at the higher end of the environmental pH values. For instance, surface water during summer can have pH > 8.5 because of photosynthetic activity (Callieri et al., 2012; Christensen et al., 2013).

**Laser flash photolysis experiments.** Flash photolysis runs were carried out using the third harmonic (355 nm) of a Quanta Ray GCR 130-01 Nd:YAG laser system instrument, used in a right-angle geometry with respect to the monitoring light beam. The single pulses energy was set to 35 mJ unless otherwise stated. A 3 mL solution volume was placed in a quartz cuvette (path length of 1 cm) and used for a maximum of four consecutive laser shots. The transient absorbance at the pre-selected wavelength was monitored by a detection system consisting of a pulsed xenon lamp (150 W), monochromator and a photomultiplier (1P28). A spectrometer control unit was used for synchronising the pulsed light source and programmable shutters with the laser output. The signal from the photomultiplier was digitised by a programmable digital oscilloscope (HP54522A). A 32 bits RISC-processor kinetic spectrometer workstation was used to analyse the digitised signal.

BZT was laser irradiated in the presence of anthraquinone-2-sulphonate (AQ2S) and 1-nitronaphthalene (1NN) as triplet sensitizers. Because of the BZT acid-base equilibrium, the experiments were carried out at pH 4 and 11 where the neutral and deprotonated forms prevail, respectively. The solution pH was set by using HClO<sub>4</sub> or NaOH. The AQ2S runs were carried out with 0.1 mM AQ2S, varying BZT concentration between 0 and 2 mM. The decay of the AQ2S triplet (<sup>3</sup>AQ2S\*) signal was monitored at different BZT concentration values, and the measured pseudo-first order decay constant  $k_{^3AQ2S^*}$  was plotted as a function of [BZT]. The slopes of the  $k_{^3AQ2S^*}$  vs. [BZT] lines were used to obtain the second-order reaction rate constants between BZT and <sup>3</sup>AQ2S\* at both pH values ( $k_{HBZT,^3AQ2S^*}$  at pH 4 and  $k_{BZT^-,^3AQ2S^*}$  at pH 11, units of M<sup>-1</sup> s<sup>-1</sup>). The second-order rate constants with the 1NN triplet state,  $k_{HBZT,^31NN^*}$  at pH 4 and  $k_{BZT^-,^31NN^*}$  at pH 11, were measured with a similar procedure using 55 μM 1NN and 0-5 mM BZT.

**Irradiation experiments.** The intermediates of HBZT and BZT<sup>-</sup> were studied upon transformation by direct photolysis, •OH reaction (10 mM H<sub>2</sub>O<sub>2</sub> as •OH source) and triplet sensitization (0.1 mM

AQ2S as triplet sensitizer). The BZT solutions (1 mM initial concentration) were irradiated in a homemade photoreactor, contained in a cylindrical stainless steel housing. Six fluorescent lamps (Philips TL D15W/05, with emission spectrum ranging from 300 to 500 nm and emission maximum at 365 nm) were positioned at regular distances around the irradiated solution, which was placed in a Pyrex tube of 2.6 cm internal diameter at the centre of the set-up. The lamps emission spectrum up to 425 nm is reported in **Figure 1**, which also shows the absorption spectra of the BZT solutions at pH 4.0 (HBZT) and 11.0 (BZT<sup>-</sup>). The lamps irradiance spectrum was recorded using a fibre optics coupled with a charge-coupled device (CCD) spectrophotometer (Ocean Optics USD 2000C UV-VIS). Note that the Pyrex glass tube would totally filter radiation below 280 nm. The used lamps are able to photoexcite H<sub>2</sub>O<sub>2</sub>, which has an absorption tail above 300 nm, as well as AQ2S that has an absorption maximum around 330 nm (Maurino et al., 2008; Nissenson et al., 2010). The limited overlap between the lamp emission and the HBZT/BZT<sup>-</sup> absorption spectra was compensated for by irradiating the relevant solutions for up to 24 h in the direct photolysis experiments. By comparison, the H<sub>2</sub>O<sub>2</sub>-containing systems were irradiated for up to 4 h and the AQ2S ones for up to 90 min. The UV irradiance of the lamps was approximately 1.5 times lower compared to the irradiance of sunlight during summertime at mid latitude (Frank and Klöppfer, 1988; Vione et al., 2009). Note, however, that the described irradiation set-up was only used to obtain qualitative and semi-quantitative information concerning the nature of the transformation intermediates, and not to assess the phototransformation kinetics of BZT in the natural environment.

The total volume of each irradiated solution was 100 mL, and all the experiments were carried out at room temperature (293±2 K). The solution pH was either 4 or 11, adjusted with HClO<sub>4</sub> or NaOH. Sample aliquots were taken from the reaction tube at scheduled time intervals, and they were characterised by Liquid Chromatography interfaced with Mass Spectrometry (LC-MS). It was used a Waters Alliance instrument equipped with an electrospray interface (used in ESI+ mode) and a Q-TOF mass spectrometer (Micromass, Manchester, UK). The capillary needle voltage was 3 kV and the source temperature 100° C. The cone voltage was set to 35 V. Data acquisition was carried out with a Micromass MassLynx 4.1 data system.

Samples were eluted with a mixture of acetonitrile (A) and 0.1% formic acid in water (B) at 0.2 mL min<sup>-1</sup> flow rate, with the following gradient: start at 5% A, then up to 95% A in 15 min, keep for 10 min, back to 5% A in 1 min and keep for 5 min (post-run equilibration). It was used a column Phenomenex Kinetex C18 (2.1 mm × 100 mm × 2.6 μm) and the retention times of BZT and aniline were 7.2 and 1.3 min, respectively (checked by using commercial standards). After the column, the eluate was monitored with a diode array detector (DAD) before the ESI-MS interface. BZT was detected at 270 nm and aniline at 254 nm. The best Limit of Detection (LOD) for aniline with this analytical set-up was 5 μM.

**Photochemical modelling.** The modelling of BZT phototransformation in surface waters was carried out with the APEX software (Aqueous Photochemistry of Environmentally-occurring Xenobiotics). APEX predicts photochemical half-life times as a function of water chemistry and

depth, for compounds with known photochemical reactivity. The relevant photochemical reactivity parameters are direct photolysis quantum yields, absorption spectra, and second-order reaction rate constants with the photogenerated transient species (Vione, 2014; Bodrato and Vione, 2014). APEX is based on a photochemical model that has been validated by comparison with light-induced transformation kinetics in surface freshwaters (Maddigapu et al., 2011; Marchetti et al., 2013; Bodrato and Vione, 2014).

The formation and decay of the main photoinduced transients ( $\bullet\text{OH}$ ,  $^1\text{O}_2$ ,  $^3\text{CDOM}^*$ ) was modelled by considering average formation quantum yields in natural waters and average inactivation rate constants, the latter by reactions with DOM and inorganic carbon (for  $\bullet\text{OH}$ ), collision with the solvent (for  $^1\text{O}_2$ ) and thermal deactivation as well as reaction with  $\text{O}_2$  (for  $^3\text{CDOM}^*$ ). The combination of formation and transformation kinetics allowed the relevant steady-state concentrations to be determined. For instance, when considering 5 m water depth, 0.1 mM nitrate, 1  $\mu\text{M}$  nitrite, 1 mM bicarbonate, 10  $\mu\text{M}$  carbonate and 1 nM bromide, with dissolved organic carbon (DOC) varying in the range from 1 to 10  $\text{mg C L}^{-1}$ ,  $[\bullet\text{OH}]$  would vary between  $10^{-16}$  and  $10^{-17}$  M, while  $[^1\text{O}_2]$  and  $[^3\text{CDOM}^*]$  would reach some  $10^{-16}$  M units.

Sunlight irradiance is not constant in the natural environment, because of meteorological issues (not included in APEX) and of diurnal and seasonal cycles. To allow easier comparison between model results and environmental conditions, APEX uses as time unit a summer sunny day (SSD), equivalent to fair-weather 15 July at  $45^\circ$  N latitude. Sunlight is not vertically incident over the water surface, but refraction at the interface deviates the light path in water towards the vertical. The light path length  $l$  depends on the depth  $d$ : on 15 July at  $45^\circ\text{N}$  it is  $l = 1.05 d$  at noon, and  $l = 1.17 d$  at  $\pm 3$  h from noon that is a reasonable daily average (Bodrato and Vione, 2014).

To model the behaviour of the two BZT forms as a function of pH, the first-order degradation rate constants of acidic and basic BZT ( $k_1$  and  $k_2$ , respectively) were calculated separately and then combined as the weighted sum of the rate constants times the relevant molar fractions ( $\alpha_{\text{HBZT}}$  and  $\alpha_{\text{BZT}^-}$ , respectively), taking into account the acid-base equilibrium with  $\text{pK}_a = 8.4$ . The combined BZT rate constant was  $k_{12} = k_1 \alpha_{\text{HBZT}} + k_2 \alpha_{\text{BZT}^-}$ . The overall BZT half-life time was then calculated as  $t_{1/2}^{\text{BZT}} = \ln 2 (k_{12})^{-1}$  (De Laurentiis et al., 2013).

## Results and Discussion

### *Laser flash photolysis experiments*

The reactivity of the acidic (HBZT) and basic (BZT $^-$ ) forms of BZT was studied upon laser irradiation of AQ2S and 1NN as triplet sensitisers, at pH 4 (HBZT) and 11 (BZT $^-$ ). The time evolution of  $^3\text{AQ2S}^*$  was monitored at 380 nm at pH 4 and at 450 nm at pH 11. The choice of the latter wavelength was motivated by the considerable 380-nm spectral interferences occurring at pH 11, which are probably accounted for by the AQ2S radical anion (AQ2S $^{\bullet-}$ ) (Hulme et al., 1972).



The  $^3\text{1NN}^*$  signal was always monitored at 620 nm. In all the cases the signal decay followed pseudo-first order kinetics. **Figure 2** reports the trends of the first-order decay constants of  $^3\text{AQ2S}^*$  and  $^3\text{1NN}^*$  as a function of BZT concentration at both pH values (Stern-Volmer plots). The figure shows linear trends under all conditions and, according to the Stern-Volmer approach, the line slopes represent the second-order reaction rate constants between the relevant BZT form and the triplet state. For HBZT (pH 4) it was found  $k_{\text{HBZT},^3\text{AQ2S}^*} = (1.84 \pm 0.23) \cdot 10^9 \text{ M}^{-1} \text{ s}^{-1}$  and  $k_{\text{HBZT},^3\text{1NN}^*} = (1.91 \pm 0.10) \cdot 10^7 \text{ M}^{-1} \text{ s}^{-1}$  (hereafter, error bounds represent  $\pm\sigma$ ). In contrast, similar reactivity values were found with  $\text{BZT}^-$  (pH 11):  $k_{\text{BZT}^-,^3\text{AQ2S}^*} = (1.67 \pm 0.13) \cdot 10^9 \text{ M}^{-1} \text{ s}^{-1}$  and  $k_{\text{BZT}^-,^3\text{1NN}^*} = (1.54 \pm 0.16) \cdot 10^9 \text{ M}^{-1} \text{ s}^{-1}$ . The higher reactivity of  $\text{BZT}^-$  compared to HBZT towards  $^3\text{1NN}^*$  suggests that  $\text{BZT}^-$  is easier to be oxidised than the protonated molecule. Because  $^3\text{AQ2S}^*$  is a stronger oxidant than  $^3\text{1NN}^*$ , as already discussed, it is not surprising to find large differences in the  $^3\text{1NN}^*$  reaction rate constants and much smaller differences in the case of  $^3\text{AQ2S}^*$ .

A summary of the BZT photoreactivity parameters is provided in **Table 1**. The direct photolysis quantum yields and the reaction rate constants with  $\bullet\text{OH}$  and  $^1\text{O}_2$  were derived from the literature, while the triplet-sensitised reactivity was determined in this work. There are different literature reports concerning the  $\text{BZT} + \bullet\text{OH}$  reactivity data, and they show a very reasonable agreement. Naik and Moorthy (1995) determined the second-order  $\bullet\text{OH}$  reaction rate constants of HBZT and  $\text{BZT}^-$  (**Table 1**), while Janssen et al. (2015) measured the lumped rate constant at pH 7.5 where BZT occurs as a mixture of HBZT and  $\text{BZT}^-$ . The value reported by Janssen et al. (2015),  $(8.3 \pm 0.1) \cdot 10^9 \text{ M}^{-1} \text{ s}^{-1}$ , is intermediate between those reported for the HBZT and  $\text{BZT}^-$  forms (Naik and Moorthy, 1995).

### *Modelling the photochemical fate of BZT in surface waters*

The values of the photoreactivity parameters shown in **Table 1**, together with the absorption spectra of HBZT and  $\text{BZT}^-$ , were used to model the phototransformation of BZT in surface waters. The main uncertainty in BZT photoreactivity is the  $\sim 2$  orders of magnitude difference between the HBZT reaction rate constants with  $^3\text{1NN}^*$  and  $^3\text{AQ2S}^*$  ( $k_{\text{HBZT},^3\text{1NN}^*}$  and  $k_{\text{HBZT},^3\text{AQ2S}^*}$ , see **Table 1**).

This large variation was taken into account in photochemical modelling. **Figure 3a** reports the half-life time ( $t_{1/2}$ ) of HBZT, as a function of the dissolved organic carbon (DOC) and of the reaction rate constant between HBZT and  $^3\text{CDOM}^*$ ,  $k_{\text{HBZT},^3\text{CDOM}^*}$  (see the caption for other water conditions). The rate constant  $k_{\text{HBZT},^3\text{CDOM}^*}$  was let to vary in a range included between  $2 \cdot 10^7$  and  $2 \cdot 10^9 \text{ M}^{-1} \text{ s}^{-1}$ . The lower limit corresponded to the value of  $k_{\text{HBZT},^3\text{1NN}^*}$ , the upper limit was just slightly higher than  $k_{\text{HBZT},^3\text{AQ2S}^*}$ . It is apparent that the value of  $k_{\text{HBZT},^3\text{CDOM}^*}$  affects both the predicted HBZT half-life times and their trend with the DOC. If  $k_{\text{HBZT},^3\text{CDOM}^*} \sim k_{\text{HBZT},^3\text{1NN}^*}$ , one observes a considerable increase of  $t_{1/2}$  with increasing DOC. In contrast, if  $k_{\text{HBZT},^3\text{CDOM}^*} \sim k_{\text{HBZT},^3\text{AQ2S}^*}$ ,  $t_{1/2}$  monotonically increases with DOC before reaching a plateau above  $2 \text{ mg C L}^{-1}$ .

To account for the reported trends, one should consider that high-DOC waters are rich in dissolved organic matter (DOM), including its chromophoric fraction (CDOM). The latter is the only source of  $^3\text{CDOM}^*$  and an important  $\bullet\text{OH}$  producer, but DOM is the key  $\bullet\text{OH}$  scavenger. Typically, the steady-state  $[\text{}^3\text{CDOM}^*]$  would increase and  $[\bullet\text{OH}]$  decrease with increasing DOC (Vione et al., 2014). Moreover, CDOM would compete with HBZT for sunlight irradiance and inhibit its direct photolysis. Usually, the extent by which the direct photolysis processes are inhibited by CDOM is lower than the extent by which the  $\bullet\text{OH}$  reactions are inhibited by DOM (Liang et al, 2015). Compared to the direct photolysis,  $\bullet\text{OH}$  reactions would thus be favoured at low DOC and  $^3\text{CDOM}^*$  reactions at high DOC. An additional issue is that the importance of the reaction between HBZT and  $^3\text{CDOM}^*$  would increase with increasing  $k_{\text{HBZT},^3\text{CDOM}^*}$ .

To better make this point, a quantitative insight into the DOC trends of the different photoprocesses, in terms of the fraction of HBZT transformation accounted for by each photoreaction pathway, is reported in **Figure 4** (**4a**:  $k_{\text{HBZT},^3\text{CDOM}^*} = k_{\text{HBZT},^3\text{1NN}^*}$ ; **4b**:  $k_{\text{HBZT},^3\text{CDOM}^*} = k_{\text{HBZT},^3\text{AQ2S}^*}$ ). The figure shows that  $^1\text{O}_2$  plays a negligible role in phototransformation, and that the  $\bullet\text{OH}$  fraction decreases and the  $^3\text{CDOM}^*$  fraction increases with DOC. The  $^3\text{CDOM}^*$  process is highly enhanced if  $k_{\text{HBZT},^3\text{CDOM}^*} = k_{\text{HBZT},^3\text{AQ2S}^*}$ , compared to  $k_{\text{HBZT},^3\text{CDOM}^*} = k_{\text{HBZT},^3\text{1NN}^*}$ . Moreover, the direct photolysis fraction has a maximum with DOC (vide infra for the rationale). Given the assumed values for the other water parameters, at  $1 \text{ mg C L}^{-1}$  DOC,  $0.1 \text{ mM}$  nitrate would account for  $\sim 50\%$  of  $\bullet\text{OH}$  photoproduction,  $1 \text{ }\mu\text{M}$  nitrite for  $\sim 30\%$ , and CDOM for  $\sim 20\%$ . In the same conditions, DOM would scavenge  $\sim 85\%$  of  $\bullet\text{OH}$ , and inorganic carbon would consume the remaining fraction. At  $10 \text{ mg C L}^{-1}$  DOC, most of the  $\bullet\text{OH}$  photoproduction would be accounted for by CDOM ( $\sim 85\%$ ), with secondary contributions from nitrate ( $\sim 10\%$ ) and nitrite ( $\sim 5\%$ ). Moreover, DOM would scavenge over  $98\%$  of  $\bullet\text{OH}$ . Bromide at typical freshwater levels (nM concentration or lower, as hypothesised in these simulations) would be a minor  $\bullet\text{OH}$  scavenger. In contrast,  $0.8 \text{ mM}$  bromide as per the typical seawater conditions would be the main dissolved species to consume  $\bullet\text{OH}$  (Mopper and Zhou, 1990). In seawater, the steady-state  $[\bullet\text{OH}]$  and the importance of the related processes would be much lower than in freshwater. For bromide to be a comparable  $\bullet\text{OH}$  scavenger as DOM, one needs a ratio  $[\text{Br}^-] \text{ DOC}^{-1} \sim 5 \cdot 10^{-6} \text{ mol Br}^- (\text{mg C})^{-1}$  (Buxton et al., 1988).

Coming back to the trends highlighted in **Figure 3a**, if  $k_{\text{HBZT},^3\text{CDOM}^*}$  is low the inhibition by (C)DOM of the direct photolysis and the  $\bullet\text{OH}$  reaction explains the large increase of  $t_{1/2}$  with DOC. In such a case, the HBZT half-life time would approach the year scale at high DOC (the actual  $t_{1/2}$  would be even longer, because the scale of the modelled half-life times is in summer sunny days). If, on the contrary,  $k_{\text{HBZT},^3\text{CDOM}^*}$  is high, the  $^3\text{CDOM}^*$  process accounts for the  $t_{1/2}$  plateau at high DOC. Moreover, if the DOC is low, the HBZT degradation by  $^3\text{CDOM}^*$  is hardly important and  $t_{1/2}$  has a limited dependence on  $k_{\text{HBZT},^3\text{CDOM}^*}$ . In contrast, if the DOC is high, there is a  $\sim 5$ -fold difference in  $t_{1/2}$  between the scenarios of  $k_{\text{HBZT},^3\text{CDOM}^*} \sim k_{\text{HBZT},^3\text{1NN}^*}$  and  $k_{\text{HBZT},^3\text{CDOM}^*} \sim k_{\text{HBZT},^3\text{AQ2S}^*}$ .

Based on similar considerations, one can explain the trend of the fraction of HBZT phototransformation accounted for by direct photolysis ( $\eta_{\text{DP}}^{\text{HBZT}}$ ), as a function of DOC and of

$k_{HBZT,^3CDOM^*}$  (**Figure 3b**). The direct photolysis fraction would reach the highest values (~7% of total phototransformation) for  $k_{HBZT,^3CDOM^*} \sim k_{HBZT,^31NN^*}$ , under which circumstances the  $^3CDOM^*$  process would be of lesser importance. The role of  $^3CDOM^*$  would also be limited at low DOC where, coherently,  $\eta_{DP}^{HBZT}$  is poorly dependent on  $k_{HBZT,^3CDOM^*}$ . To account for the maximum of  $\eta_{DP}^{HBZT}$  as a function of the DOC, one should consider the three main processes involved in HBZT phototransformation ( $\bullet OH$ , direct photolysis and  $^3CDOM^*$ ). The maximum is due to the fact that, compared to the direct photolysis, the  $\bullet OH$  reaction is favoured at low DOC and the  $^3CDOM^*$  one at high DOC (Vione et al., 2014).

**Figure 3c** shows the modelled half-life time of the dissociated form  $BZT^-$ , as a function of the DOC and the water column depth  $d$ . For the anionic form it was used  $k_{BZT^-,^3CDOM^*} = 1.6 \cdot 10^9 \text{ M}^{-1} \text{ s}^{-1}$ , as the average of the very similar values  $k_{BZT^-,^3AQ2S^*}$  and  $k_{BZT^-,^31NN^*}$ . Depending on the conditions, the modelled  $t_{1/2}$  would vary from a few days to a couple of months. The  $BZT^-$  direct photolysis can be neglected, because  $\eta_{DP}^{BZT^-} < 1\%$  under all circumstances. A similar consideration holds for the  $^1O_2$  reaction, thus  $\bullet OH$  and  $^3CDOM^*$  would be the main photoreaction pathways involved in the degradation of  $BZT^-$ .

The reaction of  $BZT^-$  with  $\bullet OH$  is expected to prevail at low DOC and that with  $^3CDOM^*$  at high DOC (Vione et al., 2014). The sharp increase of  $t_{1/2}(BZT^-)$  with increasing DOC, for  $DOC < 2 \text{ mg C L}^{-1}$ , suggests that the  $\bullet OH$  scavenging by DOM is not totally compensated for by the photoreactivity of CDOM. The reason is that the radiation absorption by CDOM rapidly reaches saturation, especially in deep waters, which limits the CDOM-induced photoreactions. In contrast, the  $\bullet OH$  scavenging by DOM increases linearly with DOC (Minella et al., 2013). **Figure 3c** also shows that the  $t_{1/2}$  of  $BZT^-$  increases with increasing depth, because the bottom layers of deep water bodies are scarcely illuminated by sunlight (Loiselle et al., 2008). Therefore, the importance of photochemical reactions is decreased in deep water columns.

**Figure 5** reports the half-life times of BZT (both forms in equilibrium), as a function of pH and of  $k_{HBZT,^3CDOM^*}$  (DOC was assumed constant at  $5 \text{ mg C L}^{-1}$ ). Note that HBZT would prevail at  $pH < 8.4$  and  $BZT^-$  at higher pH. This figure, as well as a comparison between **Figures 3a and 3c**, suggests that the  $t_{1/2}$  values of HBZT and  $BZT^-$  would be similar if  $k_{HBZT,^3CDOM^*} \sim k_{HBZT,^3AQ2S^*}$ . Under these circumstances,  $k_{HBZT,^3CDOM^*}$  would not be much different from  $k_{BZT^-,^3CDOM^*}$ , and the water pH would not be a key factor to control the photochemical persistence of BZT. In contrast, for low  $k_{HBZT,^3CDOM^*}$ , one gets that HBZT would be considerably more photostable than  $BZT^-$ . In this case, the half-life times would decrease remarkably with increasing pH.

The laser flash photolysis experiments suggested that the triplet sensitisation rate constants of HBZT and  $BZT^-$  were similar in the presence of a strongly oxidising triplet such as  $^3AQ2S^*$ , while there can be large differences with a triplet state of lower oxidising potential. In the case of surface-water CDOM, the triplet states formed by irradiation of organic matter of different origin may show different photoreactivity (Guerard et al., 2009). Note for instance that humic substances are likely to be the most photoactive CDOM components (Coelho et al., 2011), and the low molecular weight

humic fraction is more photoactive than the high molecular weight one (Richard et al., 2004). Therefore, the less photoreactive is CDOM, the more marked is the expected effect of pH on BZT photoattenuation in surface-water environments.

Overall, the modelled half-life times of BZT in different surface-water conditions would range from some days/weeks to several months or higher. In several cases, photochemistry would be more competitive than biodegradation as a BZT attenuation pathway.

### ***Photochemical transformation intermediates***

First of all, the possible formation of aniline was assessed via the main BZT phototransformation routes of environmental significance: HBZT direct photolysis (under UVB+UVA irradiation) and reaction with  $\bullet\text{OH}$  and  $^3\text{CDOM}^*$ , as well as  $\text{BZT}^-$  reaction with  $\bullet\text{OH}$  and  $^3\text{CDOM}^*$ . Aniline was always below the detection limit of the used analytical method and, therefore, the photochemical transformation of  $10^{-3}$  M HBZT or  $\text{BZT}^-$  yielded less than  $5 \cdot 10^{-6}$  M aniline. In contrast, several BZT hydroxyderivatives were detected as the transformation intermediates of HBZT and  $\text{BZT}^-$ . Their tentative structures are listed in **Table 2**, together with the main ions occurring in the mass spectra and the reaction conditions in which the relevant compounds were detected.

The identification of the intermediates as hydroxyderivatives relies on the fact that their  $m/z$  signals ( $[\text{M}+\text{H}]^+$ ) suggest the occurrence, with respect to the parent BZT, of one or more additional O atoms. It was unfortunately not straightforward to determine whether the OH groups of the hydroxyderivatives occurred on the benzene or the triazole ring, and the same difficulty has also been encountered in previous studies (Benitez et al., 2015). However, in the case of the monohydroxyderivatives, an OH group on the triazole ring could only be bound to the nitrogen atom not involved in the double bond (an alternative addition process should produce an hydroxylated intermediate without the double bond, which would have a different molecular mass). There could thus be only one monohydroxyderivative with  $m/z$  ( $[\text{M}+\text{H}]^+$ ) = 136 and the OH group on the triazole ring, to be compared with the detection of two different monohydroxylated isomers (**I** and **II**). Therefore, it is very likely that hydroxylation occurred on the benzenic ring in at least one of the two cases. Furthermore, when considering for instance the mass spectrum of **I**, the fragments at  $m/z$  110 and 94 can be tentatively explained by benzenic ring fragmentation with loss of the groups  $\text{C}_2\text{H}_2$  and  $\text{C}_2\text{HOH}$ , respectively. The loss of  $\text{C}_2\text{HOH}$  would suggest the occurrence of a OH group on the benzenic ring, although it is not possible to determine its exact location.

The  $m/z$  ( $[\text{M}+\text{H}]^+$ ) values of the intermediates **III**, **IV** and **V** suggest the occurrence of two or three additional O atoms compared to the parent BZT. The addition of more than one OH group to the triazole ring should break the  $\text{N}=\text{N}$  double bond and, in the case for instance of the dihydroxyderivative **III**, a signal  $m/z$  ( $[\text{M}+\text{H}]^+$ ) = 154 should be observed instead of 152. Therefore, no more than one OH group could be located on the triazole ring. Similar considerations apply to the trihydroxylated compounds **IV** and **V**. The spectra of the latter intermediates show fragments at  $m/z$  136 and 110, which could be consistent with the loss of  $\text{H}_2\text{NO}^\bullet$  and  $\text{C}_2\text{H}_2\text{O}_2$ . Such a

fragmentation pathway would suggest monohydroxylation of the triazole ring (at the N atom not involved in the double bond) and the occurrence of two adjacent OH groups on the benzenic ring.

In contrast, the fact that **VI** has  $m/z$  ( $[M+H]^+$ ) = 170 (two mass units higher than **IV** or **V**, see **Table 2**) could be consistent with an addition process to the N=N double bond, which could be carried out by the  $\bullet$ OH radical when present. Upon further reaction with another  $\bullet$ OH, or with  $HO_2\bullet$  as hydrogen donor (the latter can be formed easily in  $\bullet$ OH-induced degradations in aerated solution; Pan et al., 1993), one or two OH groups could be added to the N atoms previously involved in the double bond. A transformation of  $-N=N-$  into  $-NH-NOH-$  might be tentatively consistent with the presence of a fragment at  $m/z$  152, which suggests a loss of  $H_2O$  that would be favoured by the restoration of the N=N double bond.

The formation of BZT hydroxyderivatives may appear rather straightforward in the presence of  $\bullet$ OH, but these compounds were also detected upon direct photolysis and triplet sensitisation. In an aqueous solution, photoionisation (electron abstraction following photon absorption) or monoelectronic oxidation by a triplet sensitizer can produce a radical cation. The latter species, upon reaction with water and oxygen, can produce a hydroxyderivative in a similar way as  $\bullet$ OH (Kurata et al., 1988).

The possible environmental effects of the detected BZT phototransformation intermediates might partially depend on the position of the hydroxyl substituents. The parent BZT shows adverse effects towards target freshwater organisms at  $mg\ L^{-1}$  levels (Pillard et al., 2001). The progressive hydroxylation leading to intermediates **I-V** could result in a moderate decrease of toxicity, so that a trihydroxy-BZT could be about ten times less toxic than BZT (Mayo-Bean et al., 2012). An exception may occur if hydroxylation involved two OH groups in para position on the benzene ring, as hydroquinones are peculiarly toxic for fish and green algae. A BZT hydroquinone could show chronic effects at sub- $mg\ L^{-1}$  levels for the latter endpoints (Mayo-Bean et al., 2012), but there is insufficient evidence to hypothesise the occurrence of hydroquinone-like structures in the detected intermediates. In the case of **VI**, an hydrazine-like structure (without the double bond) could prompt for chronic toxic effects to fish and algae at comparable or even lower levels than the parent BZT (Mayo-Bean et al., 2012).

## Conclusions

Both BZT forms, HBZT and  $BZT^-$ , would undergo reaction with  $\bullet$ OH at low DOC and with  $^3CDOM^*$  at high DOC as important phototransformation pathways in sunlit surface waters. In addition, HBZT would also be degraded by direct photolysis as a secondary pathway, accounting for up to 7% of total phototransformation. HBZT and  $BZT^-$  have comparable reaction rate constants with  $\bullet$ OH, thus their relative photostability/photolability at high DOC depends mainly on the  $^3CDOM^*$  process. A highly reactive triplet state such as that of anthraquinone-2-sulphonate has similar reaction rate constants with HBZT and  $BZT^-$ . With similar kinetics of triplet sensitisation in

surface-water environments, the two BZT forms would undergo photodegradation with comparable lifetimes. In the presence of less reactive triplet states (as is the case of  $^3\text{INN}^*$  in this work),  $\text{BZT}^-$  reacts faster than HBZT. In this scenario, the faster triplet-sensitised transformation would make  $\text{BZT}^-$  more photolabile than HBZT, particularly in high-DOC waters. The  $\text{pK}_a$  of HBZT is 8.4, thus the HBZT/ $\text{BZT}^-$  acid-base equilibrium would partially span the typical pH values of surface waters. The importance of pH as a parameter that controls the BZT phototransformation kinetics would be inversely proportional to the  $^3\text{CDOM}^*$  reactivity, which can be different in different surface-water environments. Furthermore, pH would not be a key photodegradation factor in low-DOC waters (e.g. below  $1 \text{ mg C L}^{-1}$ ), where  $^3\text{CDOM}^*$  reactions would be a secondary pathway for any value of  $k_{\text{HBZT},^3\text{CDOM}^*}$ .

With a half-life time that, depending on the conditions and on  $^3\text{CDOM}^*$  reactivity, could vary from some days/weeks to several months or higher, photodegradation would often be a competitive process compared to biodegradation, for the attenuation of BZT in sunlit surface waters. In this study, the phototransformation of HBZT and  $\text{BZT}^-$  through the main photoreaction pathways did not yield aniline as intermediate in detectable amount. The main detected intermediates were BZT hydroxyderivatives (having one to three OH groups), which would be formed by  $\bullet\text{OH}$ -induced hydroxylation or, in the absence of hydroxyl radicals, possibly by electron abstraction followed by reaction with water. These intermediates are unlikely to be much more toxic than the parent compound.

## References

- Acero, J. L., Benitez, F. J., Real, F. J., Rodriguez, E., 2015. Elimination of selected emerging contaminants by the combination of membrane filtration and chemical oxidation processes. *Water Air Soil Pollut.* 226, article 139.
- Aguera, A., 2012. Photodegradation pathways of emerging contaminants in water. In: Rizzo, L., Belgiorno, V. (eds.), *Emerging Contaminants into the Environment: Contamination Pathways and Control*. University of Salerno, Italy, p. 27-44.
- Allam, N. K., Nazeer, A. A., Ashour, E. A., 2009. A review of the effects of benzotriazole on the corrosion of copper and copper alloys in clean and polluted environments. *J. Appl. Electrochem.* 39, 961-969.
- Alotaibi, M. D., McKinley, A. J., Patterson, B. M., Reeder, A. Y., 2015. Benzotriazoles in the aquatic environment: A review of their occurrence, toxicity, degradation and analysis. *Water Air Soil Pollut.* 226, article 226.
- Anger, C. T., Sueper, C., Blumentrit, D. J., McNeill, K., Engstrom, D. R., Arnold, W. A., 2013. Quantification of triclosan, chlorinated triclosan derivatives, and their dioxin photoproducts in lacustrine sediment cores. *Environ. Sci. Technol.* 47, 1833-1843.
- Bedini, A., De Laurentiis, E., Sur, B., Maurino, V., Minero, C., Brigante, M., Mailhot, G., Vione, D., 2012. Phototransformation of anthraquinone-2-sulphonate in aqueous solution. *Photochem. Photobiol. Sci.* 11, 1445-1453.
- Benitez, F. J., Acero, J. L., Real, F. J., Roldan, G., Rodriguez, E., 2013. Photolysis of model emerging contaminants in ultra-pure water: Kinetics, by-products formation and degradation pathways. *Water Res.* 47, 870-880.
- Benitez, F. J., Acero, J. L., Real, F. J., Roldan, G., Rodriguez, E., 2015. Ozonation of benzotriazole and methylindole: Kinetic modeling, identification of intermediates and reaction mechanisms. *J. Hazard. Mater.* 282, 224-232.
- Bodrato, M., Vione, D., 2014. APEX (Aqueous Photochemistry of Environmentally occurring Xenobiotics): A free software tool to predict the kinetics of photochemical processes in surface waters. *Environ. Sci.: Processes Impacts* 16, 732-740.
- Bomhard, E. M., Herbold, B. A., 2005. Genotoxic activities of aniline and its metabolites and their relationship to the carcinogenicity of aniline in the spleen of rats. *Crit. Rev. Toxicol.* 35, 783-835.
- Brigante, M., Charbouillot, T., Vione, D., Mailhot, G., 2010. Photochemistry of 1-nitronaphthalene: A potential source of singlet oxygen and radical species in atmospheric waters. *J. Phys. Chem. A* 114, 2830-2836.
- Briguglio, I., Piras, S., Corona, P., Gavini, E., Nieddu, M., Boatto, G., Carta, A., 2015. Benzotriazole: An overview on its versatile biological behavior. *Eur. J. Med. Chem.* 96, 612-648.

- Buxton, G.V., Greenstock, C.L., Helman, W.P., Ross, A.B., 1988. Critical review of rate constants for reactions of hydrated electrons, hydrogen atoms and hydroxyl radicals ( $\bullet\text{OH}/\bullet\text{O}^-$ ) in aqueous solution. *J. Phys. Chem. Ref. Data* 17, 1027-1284.
- Callieri, C., Caravati, E., Corno, G., Bertoni, R., 2012. Picocyanobacterial community structure and space-time dynamics in the subalpine Lake Maggiore (N. Italy). *J. Limnol.* 71, 95-103.
- Careghini, A., Mastorgio, A. F., Saponaro, S., Sezenna, E., 2015. Bisphenol A, nonylphenols, benzophenones, and benzotriazoles in soils, groundwater, surface water, sediments, and food: A review. *Environ. Sci. Pollut. Res.* 22, 5711-5741.
- Carlos, L., Martire, D. O., Gonzalez, M. C., Gomis, J., Bernabeu, A., Amat, A. M., Arques, A., 2012. Photochemical fate of a mixture of emerging pollutants in the presence of humic substances. *Water Res.* 46, 4732-4740.
- Chiwa, M., Higashi, N., Otsuki, K., Kodama, H., Miyajima, T., Takeda, K., Sakugawa, H., 2015. Sources of hydroxyl radical in headwater streams from nitrogen-saturated forest. *Chemosphere* 119, 1386-1390.
- Christensen, J. P. A., Sand-Jensen, K., Staehr, P. A., 2013. Fluctuating water levels control water chemistry and metabolism of a charophyte-dominated pond. *Freshw. Biol.* 58, 1353-1365.
- Clark, C. D., de Bruyn, W., Jones, J. G., 2014. Photoproduction of hydrogen peroxide in aqueous solution from model compounds for chromophoric dissolved organic matter (CDOM). *Mar. Poll. Bull.* 79, 54-60.
- Coelho, C., Guyot, G., ter Halle, A., Cavani, L., Ciavatta, C., Richard, C., 2011. Photoreactivity of humic substances: Relationship between fluorescence and singlet oxygen production. *Environ. Chem. Lett.* 9, 447-451.
- Copper Development Association, 2016. Benzotriazole: An effective corrosion inhibitor for copper alloys. Publication #a1349, <http://www.copper.org>, last accessed January 2016.
- Cory, R. M., McKnight, D. M., 2005. Fluorescence spectroscopy reveals ubiquitous presence of oxidized and reduced quinones in dissolved organic matter. *Environ. Sci. Technol.* 39, 8142-8149.
- De Laurentiis, E., Minella, M., Maurino, V., Minero, C., Mailhot, G., Sarakha, M., Brigante, M., Vione, D., 2012. Assessing the occurrence of the dibromide radical ( $\text{Br}_2^{\bullet-}$ ) in natural waters: Measures of triplet-sensitized formation, reactivity, and modelling. *Sci. Total Environ.* 439, 299-306.
- De Laurentiis, E., Minella, M., Sarakha, M., Marrese, A., Minero, C., Mailhot, G., Brigante, M., Vione, D., 2013. Photochemical processes involving the UV absorber benzophenone-4 (2-hydroxy-4-methoxybenzophenone-5-sulphonic acid) in aqueous solution: Reaction pathways and implications for surface waters. *Water Res.* 47, 5943-5953.
- De Laurentiis, E., Prasse, C., Ternes, T. A., Minella, M., Maurino, V., Minero, C., Sarakha, M., Brigante, M., Vione, D., 2014. Assessing the photochemical transformation pathways of acetaminophen relevant to surface waters: Transformation kinetics, intermediates, and modelling. *Water Res.* 53, 235-248.



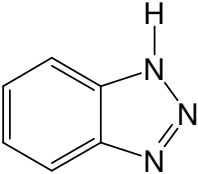
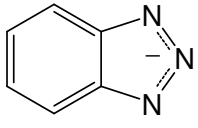
- DellaGreca, M., Fiorentino, A., Isidori, M., Lavorgna, M., Previtera, L., Rubino, M., Temussi, F., 2004. Toxicity of prednisolone, dexamethasone and their photochemical derivatives on aquatic organisms. *Chemosphere* 54, 629-637.
- EPA, 2000. Aniline Hazard Summary. <http://www3.epa.gov/airtoxics/hlthef/aniline.html>, last accessed January 2016.
- Fimmen, R. L., Cory, R. M., Chin, Y. P., Trouts, T. D., McKnight, D. M., 2007. Probing the oxidation-reduction properties of terrestrially and microbially derived dissolved organic matter. *Geochim. Cosmochim. Acta* 71, 3003-3015.
- Finsgar, M., Milosev, I., 2010. Inhibition of copper corrosion by 1,2,3-benzotriazole: A review. *Corrosion Sci.* 52, 2737-2749.
- Frank, R., Klöpffer, W., 1988. Spectral solar photo irradiance in Central Europe and the adjacent north Sea. *Chemosphere* 17, 985-994.
- Giger, W., Schaffner, C., Kohler, H. P. E., 2006. Benzotriazole and tolyltriazole as aquatic contaminants. 1. Input and occurrence in rivers and lakes. *J. Environ. Sci. Technol.* 40, 7186-7192.
- Guerard, J. J., Miller, P. L., Trouts, T. D., Chin, Y. P., 2009. The role of fulvic acid composition in the photosensitized degradation of aquatic contaminants. *Aquat. Sci.* 71, 160-169.
- Hansen, L. D., West, B. D., Baca, E. J., Blank, C. L., 1968. Thermodynamics of proton ionization from some substituted 1,2,3-triazoles in dilute aqueous solution. *J. Am. Chem. Soc.* 90, 6588-6592.
- Hem, L. J., Hartnik, T., Roseth, R., Breedveld, G. D., 2003. Photochemical degradation of benzotriazole. *J. Environ. Sci. Heal. A* 38, 471-481.
- Herzog, B., Lemmer, H., Helmreich, B., Horn, H., Mueller, E., 2014. Monitoring benzotriazoles: a 1 year study on concentrations and removal efficiencies in three different wastewater treatment plants. *Water Sci. Technol.* 69, 710-717.
- Hulme, B. E., Land, E. J., Phillip, G. O., 1972. Pulse radiolysis of 9,10-anthraquinones. Part 1. Radicals, *J. Chem. Soc., Faraday Trans. I* 68, 1992-2002.
- Janssen, E. M. L., Marron, E., McNeill, K., 2015. Aquatic photochemical kinetics of benzotriazole and structurally related compounds. *Environ. Sci.: Processes Impacts* 17, 939-946.
- Kurata, T., Watanabe, Y., Katoh, M., Sawaki, Y., 1988. Mechanism of aromatic hydroxylation in the Fenton and related reactions. One-electron oxidation and the NIH shift. *J. Am. Chem. Soc.* 110, 7472-7478.
- Lee, E., Glover, C. M., Rosario-Ortiz, F. L., 2013. Photochemical formation of hydroxyl radical from effluent organic matter: Role of composition. *Environ. Sci. Technol.* 47, 12073-12080.
- Liang, C., Zhao, H., Deng, M., Quan, X., Chen, S., Wang, H., 2015. Impact of dissolved organic matter on the photolysis of the ionizable antibiotic norfloxacin. *J. Environ. Sci. (China)* 27, 115-123.
- Liu, Y. S., Ying, G. G., Shareef, A., Kookana, R. S., 2011. Biodegradation of three selected benzotriazoles under aerobic and anaerobic conditions. *Water Res.* 45, 5005-5014.

- Liu, Y. S., Ying, G. G., Shareef, A., Kookana, R. S., 2013. Biodegradation of three selected benzotriazoles in aquifer materials under aerobic and anaerobic conditions. *J. Contam. Hydrol.* 151, 131-139.
- Loeff, I., Rabani, J., Treinin, A., Linschitz, H., 1993. Charge transfer and reactivity of  $n\pi^*$  and  $\pi\pi^*$  organic triplets, including anthraquinonesulfonates, in interactions with inorganic anions: A comparative study based on classical Marcus theory. *J. Am. Chem. Soc.* 115, 8933-8942.
- Loiselle, S. A., Azza, N., Cozar, A., Bracchini, L., Tognazzi, A., Dattilo, A., Rossi, C., 2008. Variability in factors causing light attenuation in Lake Victoria. *Freshw. Biol.* 53, 535-545.
- Maddigapu, P.R., Minella, M., Vione, D., Maurino, V., Minero, C., 2011. Modeling phototransformation reactions in surface water bodies: 2,4-Dichloro-6-nitrophenol as a case study. *Environ. Sci. Technol.* 45, 209-214.
- Marchetti, G., Minella, M., Maurino, V., Minero, C., Vione, D., 2013. Photochemical transformation of atrazine and formation of photointermediates under conditions relevant to sunlit surface waters: Laboratory measures and modelling. *Water Res.* 47, 6211-6222.
- Matamoros, V., Jover, E., Bayona, J. M., 2010. Occurrence and fate of benzothiazoles and benzotriazoles in constructed wetlands. *Water Sci. Technol.* 61, 191-198.
- Maurino, V., Borghesi, D., Vione, D., Minero, C., 2008. Transformation of phenolic compounds upon UVA irradiation of anthraquinone-2-sulfonate. *Photochem. Photobiol. Sci.* 7, 321-327.
- Mayo-Bean, K., Moran, K., Meylan, B., Ranslow, P., 2012. Methodology Document for the ECOlogical Structure-Activity Relationship Model (ECOSAR) Class Program. US-EPA, Washington DC, 46 pp.
- McNeill, K. S., Cancilla, D. A., 2009. Detection of triazole deicing additives in soil samples from airports with low, mid, and large volume aircraft deicing activities. *Bull. Environ. Contam. Toxicol.* 82, 265-269.
- Minella, M., De Laurentiis, E., Buhvestova, O., Haldna, M., Kangur, K., Maurino, V., Minero, C., Vione, D., 2013. Modelling lake-water photochemistry: three-decade assessment of the steady-state concentration of photoreactive transients ( $\cdot\text{OH}$ ,  $\text{CO}_3^{\cdot-}$  and  $^3\text{CDOM}^*$ ) in the surface water of polymictic Lake Peipsi (Estonia/Russia). *Chemosphere* 90, 2589-2596.
- Molins-Delgado, D., Diaz-Cruz, M. S., Barcelo, D., 2015. Removal of polar UV stabilizers in biological wastewater treatments and ecotoxicological implications. *Chemosphere* 119, S51-S57.
- Mopper, K., Zhou, X., 1990. Hydroxyl radical photoproduction in the sea and its potential impact on marine processes. *Science* 250, 661-664.
- Morasch, B., Bonvin, F., Reiser, H., Grandjean, D., De Alencastro, L. F., Perazzolo, C., Chevre, N., Kohn, T., 2010. Occurrence and fate of micropollutants in the Vidy Bay of Lake Geneva, Switzerland. Part II: Micropollutant removal between wastewater and raw drinking water. *Environ. Toxicol. Chem.* 29, 1658-1668.
- Naik, D. B., Moorthy, P. N., 1995. Studies on the transient species formed in the pulse radiolysis of benzotriazole. *Radiat. Phys. Chem.* 46, 353-357.

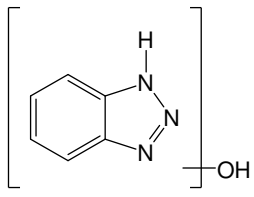
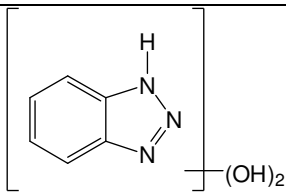
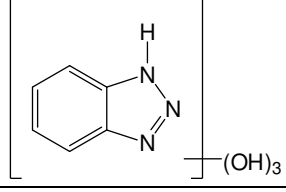
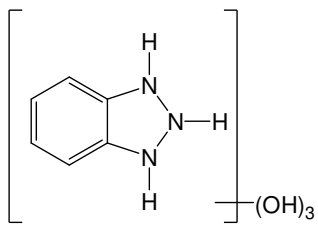
- Nakatani, N., Ueda, M., Shindo, H., Takeda, K., Sakugawa, H., 2007. Contribution of the photo-fenton reaction to hydroxyl radical formation rates in river and rain water samples. *Anal. Sci.* 23, 1137-1142.
- Nissenson, P., Dabdub, D., Das, R., Maurino, V., Minero, C., Vione, D., 2010. Evidence of the water-cage effect on the photolysis of  $\text{NO}_3^-$  and  $\text{FeOH}^{2+}$ . Implications of this effect and of  $\text{H}_2\text{O}_2$  surface accumulation on photochemistry at the air-water interface of atmospheric droplets. *Atmos. Environ.* 44, 4859-4866.
- Pan, X. M., Schuchmann, M. N., von Sonntag, C., 1993. Oxidation of benzene by the OH radical. A product and pulse radiolysis study in oxygenated aqueous solution. *J. Chem. Soc., Perkin Trans. 2*, 289-297.
- Pillard, D. A., Cornell, J. S., Dufresne, D. L., Hernandez, M. T., 2001. Toxicity of benzotriazole and benzotriazole derivatives to three aquatic species. *Water Res.* 35, 557-560.
- Reemtsma, T., Miehe, U., Duennbier, U., Jekel, M., 2010. Polar pollutants in municipal wastewater and the water cycle: Occurrence and removal of benzotriazoles. *Water Res.* 44, 596-604.
- Richard, C., Trubetskaya, O., Trubetskoj, O., Reznikova, O., Afanaseva, G., Aguer, J. P., Guyot, G., 2004. Key role of the low molecular size fraction of soil humic acids for fluorescence and photoinductive activity. *Environ. Sci. Technol.* 38, 2052-2057.
- Sulej, A. M., Polkowska, Z., Astel, A., Namiesnik, J., 2013. Analytical procedures for the determination of fuel combustion products, anti-corrosive compounds, and de-icing compounds in airport runoff water samples. *Talanta* 117, 158-167.
- Sur, B., Rolle, M., Minero, C., Maurino, V., Vione, D., Brigante, M., Mailhot, G., 2011. Formation of hydroxyl radicals by irradiated 1-nitronaphthalene (1NN): oxidation of hydroxyl ions and water by the 1NN triplet state. *Photochem. Photobiol. Sci.* 10, 1817-1824.
- Takeda, K., Takedoi, H., Yamaji, S., Ohta, K., Sakugawa, H., 2004. Determination of hydroxyl radical photoproduction rates in natural waters. *Anal. Sci.* 20, 153-158.
- Vetter, W., Lorenz, J., 2013. Determination of benzotriazoles in dishwasher tabs from Germany and estimation of the discharge into German waters. *Environ. Sci. Pollut. Res.* 20, 4435-4440.
- Vione, D., Lauri, V., Minero, C., Maurino, V., Malandrino, M., Carlotti, M. E., Olariu, R. I., Arsene, C., 2009. Photostability and photolability of dissolved organic matter upon irradiation of natural water samples under simulated sunlight. *Aquat. Sci.* 71, 34-45.
- Vione, D., 2014. A test of the potentialities of the APEX software (Aqueous Photochemistry of Environmentally-occurring Xenobiotics). Modelling the photochemical persistence of the herbicide cycloxydim in surface waters, based on literature kinetics data. *Chemosphere* 99, 272-275.
- Vione, D., Minella, M., Maurino, V., Minero, C., 2014. Indirect photochemistry in sunlit surface waters: Photoinduced production of reactive transient species. *Chemistry Eur. J.* 20, 10590-10606.
- Wang, X. H., Lin, A. Y. C., 2012. Phototransformation of cephalosporin antibiotics in an aqueous environment results in higher toxicity. *Environ. Sci. Technol.* 46, 12417-12426.

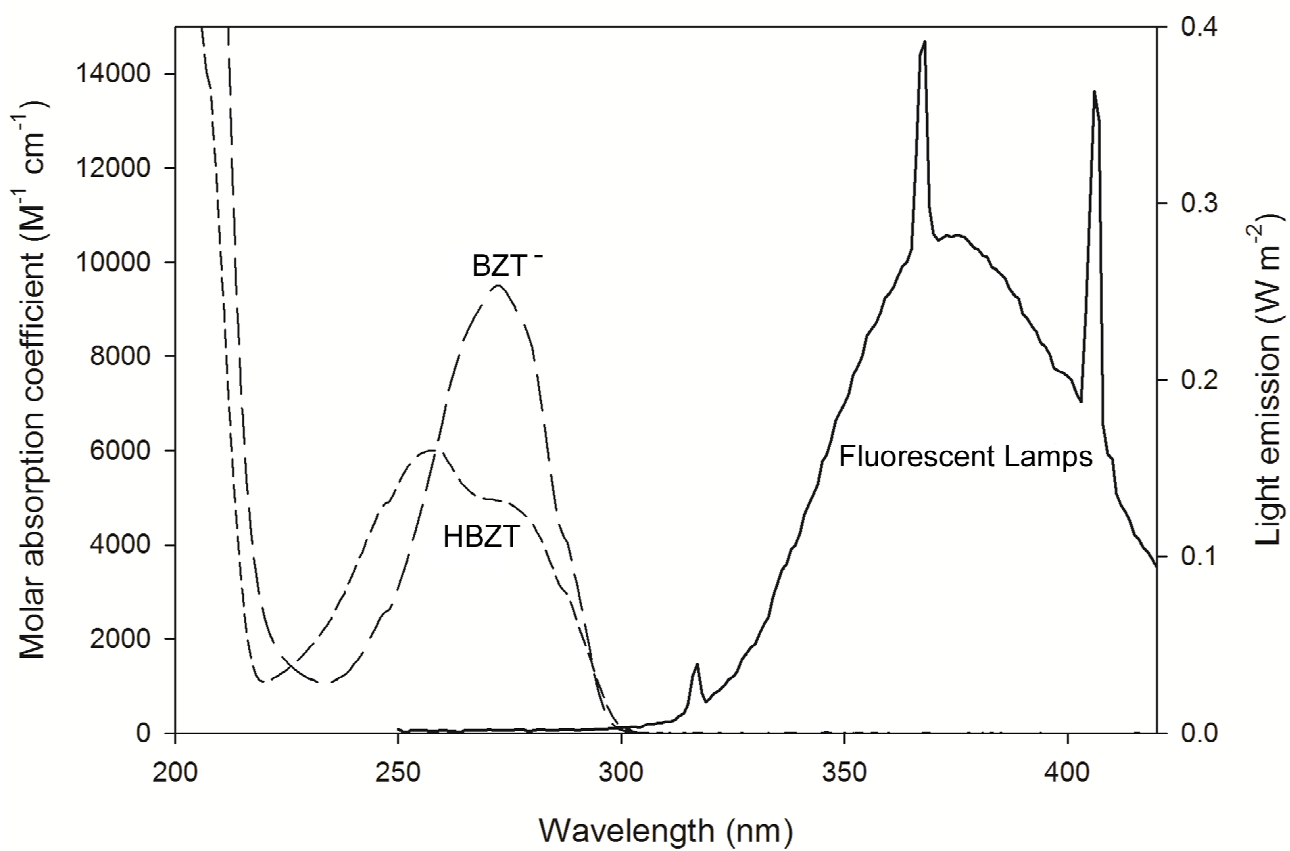
Wang, J. L., Wang, G. D., Khan, M. F., 2015. Disorder of G2-M checkpoint control in aniline-induced cell proliferation in rat spleen. Plos One 10, article e0131457.

**Table 1.** Photoreactivity parameters of HBZT and BZT<sup>-</sup>, used in photochemical modelling. Error bounds represent  $\pm\sigma$ . The data sources (literature references or this work) are also provided.

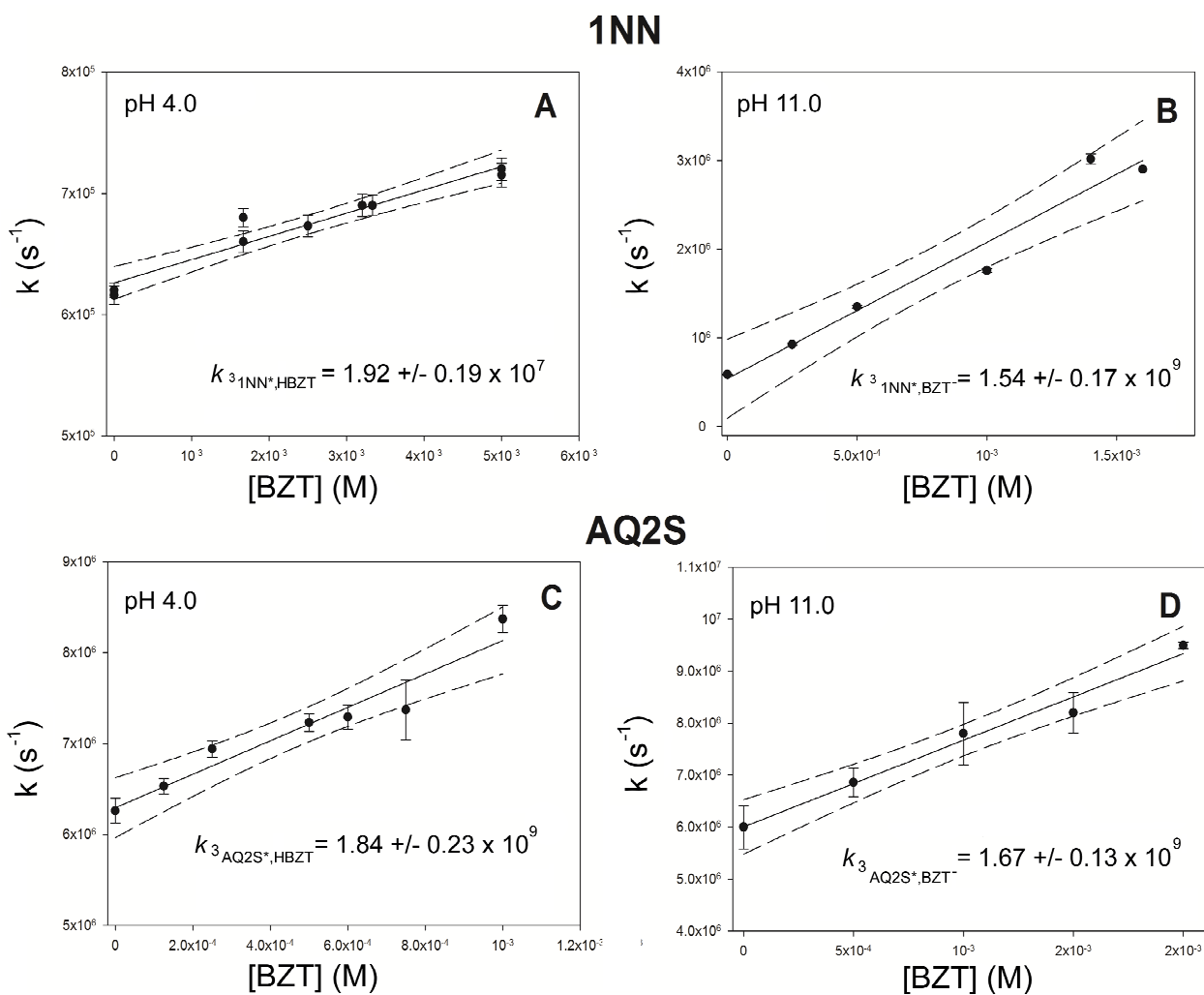
	 <b>HBZT</b>	 <b>BZT<sup>-</sup></b>	<b>Reference</b>
<b><math>\Phi</math>, unitless</b>	$(5.4\pm 0.1)\cdot 10^{-2}$	$(9.4\pm 0.1)\cdot 10^{-3}$	Benitez et al., 2013
$k_{\cdot OH}, M^{-1} s^{-1}$	$7.6\cdot 10^9$	$9.0\cdot 10^9$	Naik and Moorthy, 1995
$k_{1O_2}, M^{-1} s^{-1}$	$< 2\cdot 10^5$	$< 2\cdot 10^5$	Janssen et al., 2015
$k_{3_{1NN*}}, M^{-1} s^{-1}$	$(1.91\pm 0.10)\cdot 10^7$	$(1.54\pm 0.16)\cdot 10^9$	This work
$k_{3_{AQ2S*}}, M^{-1} s^{-1}$	$(1.84\pm 0.23)\cdot 10^9$	$(1.67\pm 0.13)\cdot 10^9$	This work

**Table 2.** Structures of the phototransformation intermediates detected in different conditions. The LC retention times and the m/z ratios of the main ions are also reported. In the structures of the intermediates, the OH group(s) could replace the hydrogen atoms at any given position (either explicit or not).

Transformation intermediate	$t_R$ , min	Ions, m/z	Conditions
	3.0 (I)	136 [M+H] <sup>+</sup> , 110, 102, 94	HBZT+hv HBZT/BZT <sup>-</sup> + <sup>•</sup> OH HBZT/BZT <sup>-</sup> + <sup>3</sup> AQ2S*
	3.8 (II)	136 [M+H] <sup>+</sup> , 102, 94	HBZT+hv HBZT+ <sup>•</sup> OH BZT <sup>-</sup> + <sup>•</sup> OH (traces) HBZT/BZT <sup>-</sup> + <sup>3</sup> AQ2S*
	2.3 (III)	152 [M+H] <sup>+</sup> , 126, 102, 94	HBZT/BZT <sup>-</sup> + <sup>•</sup> OH
	1.9 (IV)	168 [M+H] <sup>+</sup> , 136, 110, 102, 94	HBZT/BZT <sup>-</sup> + <sup>•</sup> OH
	2.0 (V)	168 [M+H] <sup>+</sup> , 136, 110, 102, 95	HBZT+ <sup>•</sup> OH BZT <sup>-</sup> + <sup>•</sup> OH (traces)
	1.7 (VI)	170 [M+H] <sup>+</sup> , 152, 126, 102, 94	HBZT+hv HBZT+ <sup>•</sup> OH BZT <sup>-</sup> + <sup>•</sup> OH (traces)

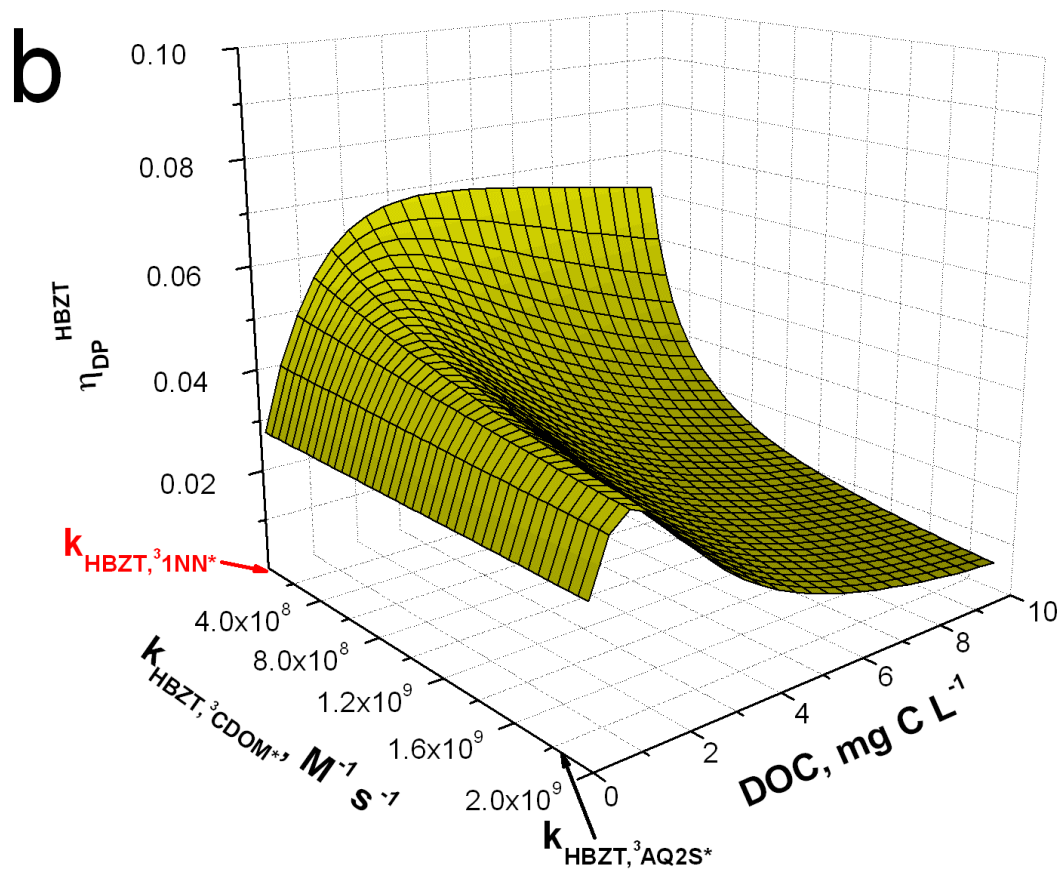
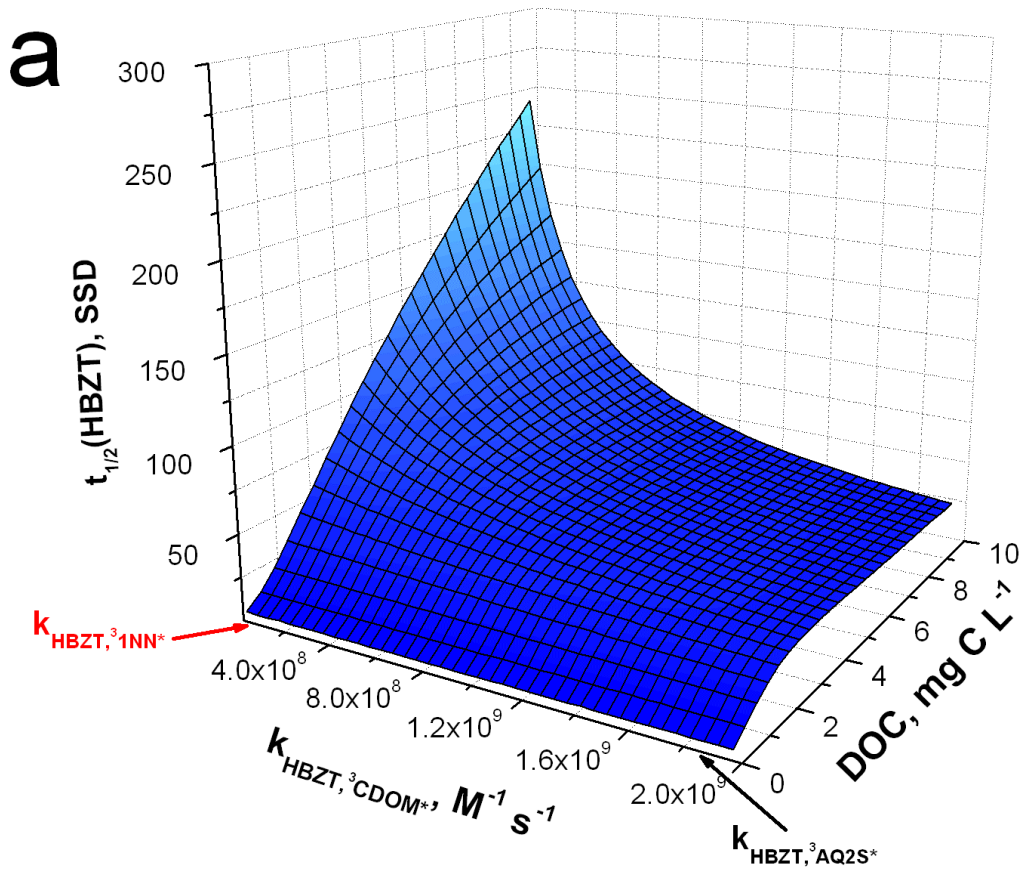


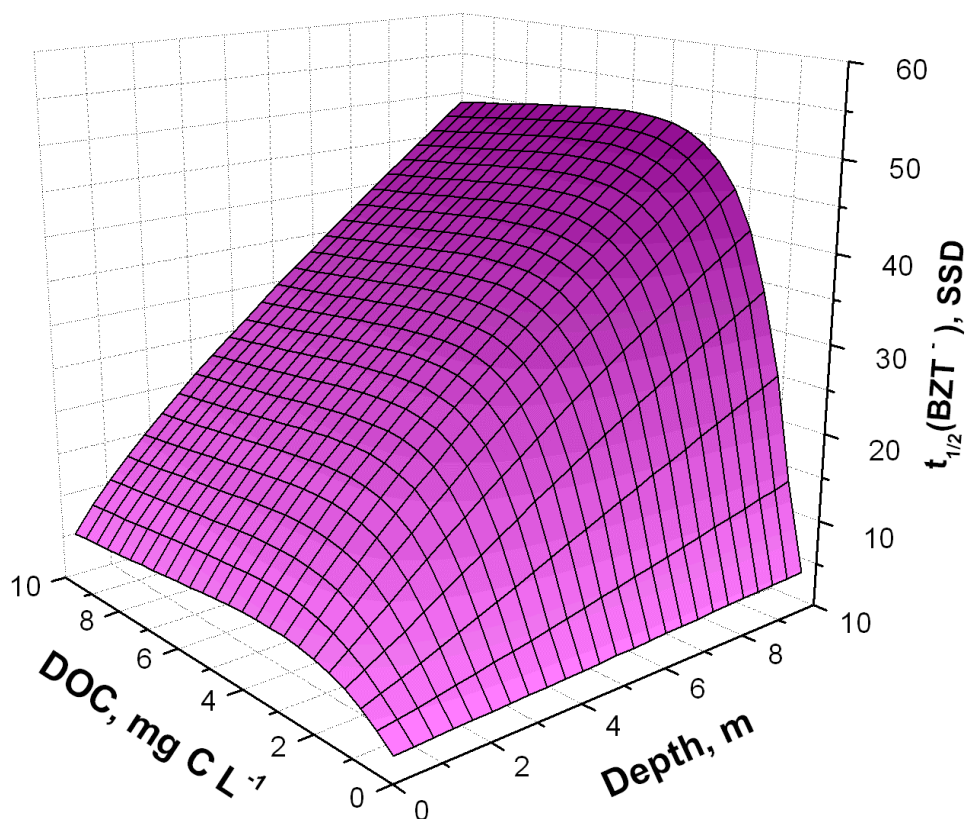
**Figure 1.** Absorption spectra (molar absorption coefficients, left Y-axis) of BZT solutions at pH 4.0 (HBZT) and 11.0 (BZT<sup>-</sup>). The right Y-axis reports the lamps irradiance spectrum.



**Figure 2.** Trends of the pseudo-first order decay constants of <sup>3</sup>1NN\* (A and B) and <sup>3</sup>AQ2S\* (C and D), at pH 4.0 (HBZT: A, C) and 11.0 (BZT<sup>-</sup>: B, D), as a function of the BZT concentration. The least-squares fit line is solid, the dashed curves are the 95% confidence limits of the fit. The value of the second-order reaction rate constant between <sup>3</sup>1NN\*/<sup>3</sup>AQ2S\* and HBZT/BZT<sup>-</sup> (slope of the least-squares line, units of M<sup>-1</sup> s<sup>-1</sup>) is reported on each relevant plot.





**C**

**Figure 3. (a)** Half-life times of HBZT, as a function of the DOC and the reaction rate constant between HBZT and <sup>3</sup>CDOM\* ( $k_{HBZT,^3CDOM^*}$ ).

**(b)** Fraction of HBZT phototransformation accounted for by direct photolysis ( $\eta_{DP}^{HBZT}$ ), as a function of DOC and  $k_{HBZT,^3CDOM^*}$ .

**(c)** Half-life times of BZT<sup>-</sup>, as a function of DOC and the water depth  $d$ .

Other water conditions in all the three cases: 5 m depth (when not varying), 0.1 mM nitrate, 1  $\mu$ M nitrite, 1 mM bicarbonate, 1 nM bromide.

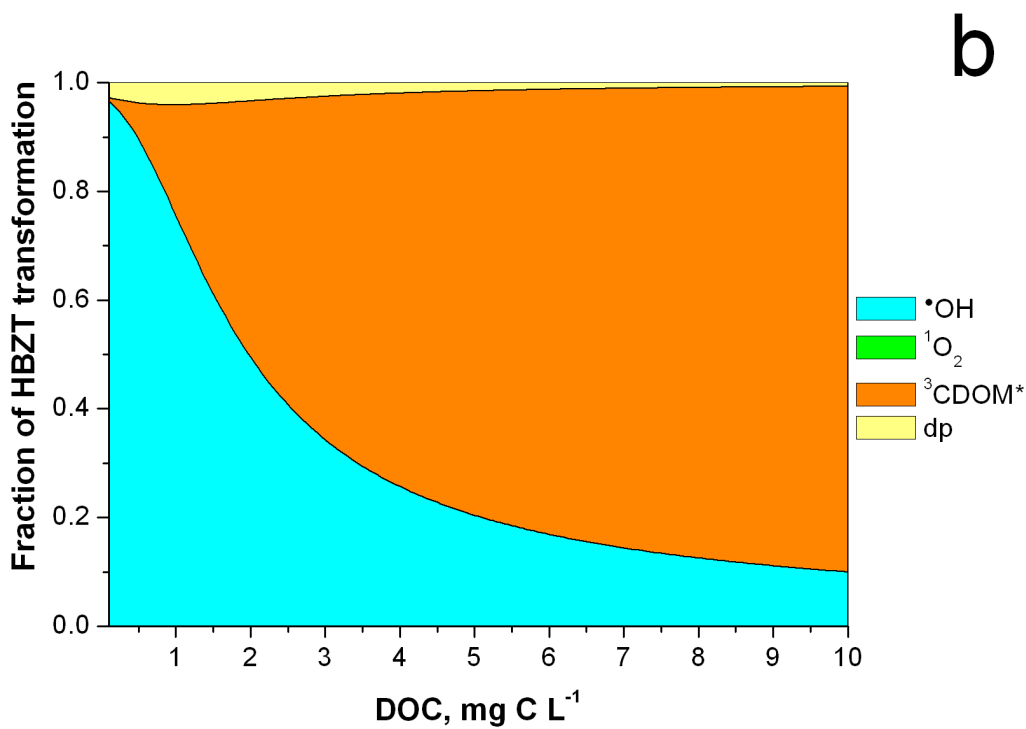
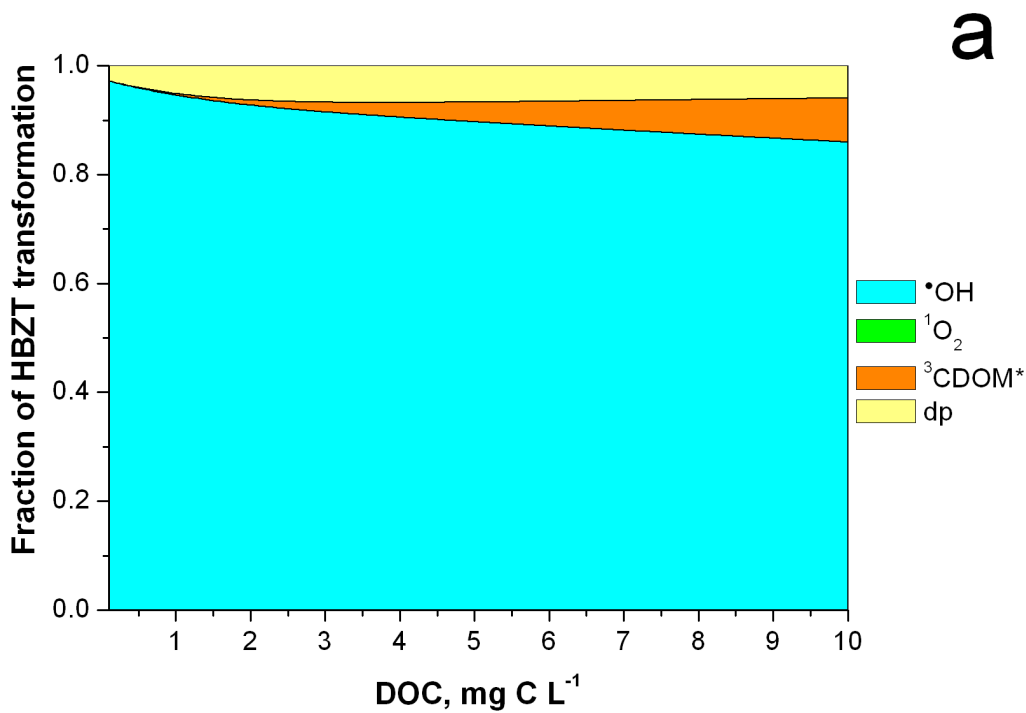


**Figure 4.** Modelled fractions of HBZT transformation accounted for by the different photoreaction pathways (dp = direct photolysis), as a function of the DOC. **(a)**  $k_{HBZT,{}^3CDOM^*} = k_{HBZT,{}^3INN^*}$ ; **(b)**  $k_{HBZT,{}^3CDOM^*} = k_{HBZT,{}^3AQ2S^*}$ . Other water conditions: 5 m depth, 0.1 mM nitrate, 1  $\mu$ M nitrite, 1 mM bicarbonate, 1 nM bromide.

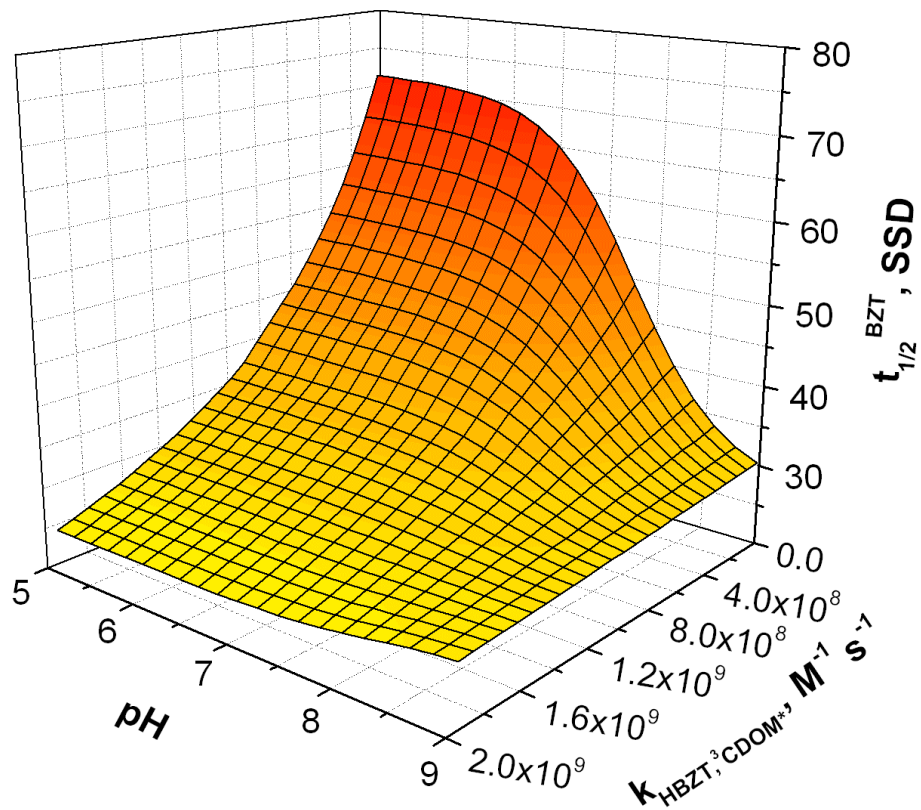


**Figure 5.** Half-life time of BZT (it includes both forms in equilibrium, HBZT and  $\text{BTZ}^-$ , with  $\text{pK}_a = 8.4$ ), as a function of pH and of the reaction rate constant between HBZT and  $^3\text{CDOM}^*$  ( $k_{\text{HBZT}, ^3\text{CDOM}^*}$ ). The corresponding  $\text{BZT}^-$  rate constant,  $k_{\text{BZT}^-, ^3\text{CDOM}^*}$ , was assumed to be  $1.6 \cdot 10^9 \text{ M}^{-1} \text{ s}^{-1}$ . Other water conditions:  $5 \text{ mg C L}^{-1}$  DOC, 5 m water depth, 0.1 mM nitrate, 1  $\mu\text{M}$  nitrite, 1 mM bicarbonate, 1 nM bromide.